J. Fluid Mech. (1967), *vol.* 29, *part* 2, *pp.* 361–372
Printed in Great Britain

A theory of water-bells

By JEAN-YVES PARLANGE

Department of Engineering and Applied Science,
Yale University, New Haven, Connecticut

(Received 17 October 1966 and in revised form 6 April 1967)

A theory is developed to determine the shape of water-bells. The motion of the gas induced by the moving walls is taken into account in this analysis. A rapidly converging iterative procedure leads to a theoretical shape which agrees well with the experimental shape of the water-bell.

1. Introduction

When a vertical jet of liquid impinges on the centre of a disk, the liquid spreads out on the disk and leaves it to form a transparent sheet that may or may not close at the bottom. When it closes, it assumes a shape as shown in figure 1, and is usually referred to as a water-bell. Clearly, the shape of the water-bell depends on the surface tension of the liquid. Indeed Boussinesq (1913) wrote Newton's law, for an element of fluid subjected to gravitational force and surface tension, and obtained equations governing the water-bell shape.

When the shape is determined experimentally, Boussinesq's equation provides a means to determine the surface tension σ. Numerous experiments have been conducted for this purpose (see references in Wegener & Parlange (1964)). However, surface tensions so determined are often much larger than those given by other experiments. Wegener & Parlange (1964) showed that if the motion of gas inside the bell generated by the liquid sheet is taken into consideration, the disagreement with other experiments disappears. In making this comparison, Wegener & Parlange (1964) took the experimental bell shape and estimated the difference $[p_0-p(s)]$ between the outside and inside pressure, induced by the gas motion. The surface tension was then computed from the amended Boussinesq's equation

$$\frac{d^2r}{dt^2} = -\frac{C}{h\rho_w}2\sigma\frac{dz}{ds} - \frac{1}{h\rho_w}[p_0-p(s)]\frac{dz}{ds}, \tag{1}$$

with

$$v(s) = [v_1^2+2g(z-z_1)]^{\frac{1}{2}}, \tag{2}$$

$$C = \frac{d(s-r\sin\phi)}{r\,dz}, \tag{3}$$

where C is the curvature; the meaning of r, s, ϕ, and z is indicated on figure 1; h is the water-layer thickness; ρ_w the water density; and subscript 1 designates a point of the sheet. The gravity term, $2g(z-z_1)$, is often negligible for small bells and high velocities $v(s)$. h is given in terms of the water flow rate $Q = 2\pi rhv(s)$.

A complete theory of water-bells, however, must include a means of computing

not only the internal motion of the air trapped within the bell but must also include the calculation of the bell shape. Such a theory is presented here. Apart from Boussinesq's original contribution, previous work on water-bells is mostly of an experimental nature. In his study of dynamics of liquid sheets, Taylor (1959) gave a theory of water-bells where the air motion inside the cavity is neglected. In his experiments the internal motion of the air is hampered by the presence of a large pipe. For such special cases one may be justified in neglecting the air motion and the term $[p_0 - p(s)]$ in equation (1) altogether.

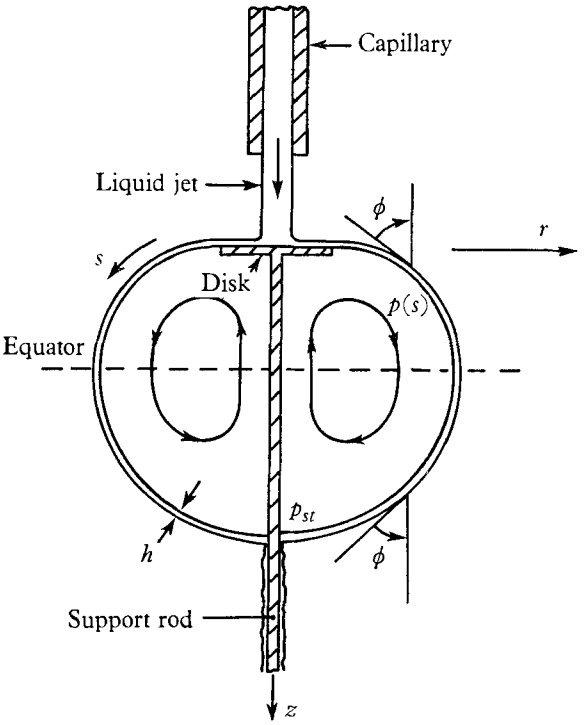

FIGURE 1. Sketch of water-bell and nomenclature.

2. The boundary value problem

As the air motion induced inside the water-bell is slow, the air may be regarded as incompressible and at a uniform temperature. Let V be the velocity of the air; ρ_a, its density; p, the pressure and ν_a the kinematic viscosity. We assume that the motion induced is axisymmetric. If ψ denotes the stream function, then the velocity components (q_z, q_r) are given by

$$q_r = \frac{1}{r}\frac{\partial \psi}{\partial z}; \quad q_z = -\frac{1}{r}\frac{\partial \psi}{\partial r}. \tag{4}$$

For axially symmetric flows the vorticity is in the azimuthal direction. Denoting this component of the vorticity by ξ we have

$$\xi = \frac{\partial q_r}{\partial z} - \frac{\partial q_z}{\partial r} = \frac{1}{r}\left[\frac{\partial^2 \psi}{\partial z^2} + \frac{\partial^2 \psi}{\partial r^2} - \frac{1}{r}\frac{\partial \psi}{\partial r}\right]. \tag{5}$$

The equation of motion may be conveniently expressed in terms of ξ/r by eliminating the pressure in the Navier–Stokes equations, thus

$$q_r\frac{\partial \xi/r}{\partial r}+q_z\frac{\partial \xi/r}{\partial z}=\nu_a\left[\frac{\partial^2\xi/r}{\partial z^2}+\frac{\partial^2\xi/r}{\partial r^2}+\frac{3}{r}\frac{\partial \xi/r}{\partial r}\right]. \tag{6}$$

Our problem is to solve the non-linear system of equations (1) to (6) subjected to the boundary condition that the velocity of air at the liquid sheet is the same as the velocity of the sheet. The location of the liquid sheet is, of course, not known *a priori*; it is governed by equation (1) and depends, among other things, on the motion of air inside the water-bell through the term $[p_0-p(s)]$. The problem is then very complicated, we shall attempt to provide a solution for an important limiting case. If D denotes a typical dimension of the water-bell (e.g. the maximum width) and V denotes a typical velocity of air at the sheet, the Reynold's number of the flow is DV/ν_a. In most cases of practical interest, this Reynold's number is large—of the order of 10^3–10^4. This means that the viscous effect is totally negligible except in a layer of thickness δ near the liquid sheet and $\delta^2 = O(D\nu_a/V)$. A solution of the boundary-value problem will be sought for the limiting case of large Reynold's number.

3. Batchelor's theorem

Batchelor (1956) proved the following theorem: in an axisymmetric flow involving closed streamlines the only solution of equation (6) satisfying the boundary condition $\xi/r = A$ on a closed streamline L' is, inside L', $\xi/r = A$. That this is a solution of the problem is evident. Batchelor showed that indeed this is the *only* solution. It is interesting that a very simple proof of Batchelor's theorem may be devised as follows. Let $\xi/r = Y$ be a second solution of (6), $Y = A$ at the boundary. That is

$$q_r(Y)\frac{\partial Y}{\partial r}+q_z(Y)\frac{\partial Y}{\partial z}=\nu_a\left[\frac{\partial^2 Y}{\partial z^2}+\frac{\partial^2 Y}{\partial r^2}+\frac{3}{r}\frac{\partial Y}{\partial r}\right],$$

$Y = A$ on L'.

Let us now define a quantity Z by $Z = Y-A$, then

$$\frac{\partial Z}{\partial r}=\frac{\partial Y}{\partial r},\quad \frac{\partial Z}{\partial z}=\frac{\partial Y}{\partial z}.$$

Z satisfies the system

$$q_r(Y)\frac{\partial Z}{\partial r}+q_z(Y)\frac{\partial Z}{\partial z}=\nu_a\left[\frac{\partial^2 Z}{\partial z^2}+\frac{\partial^2 Z}{\partial r^2}+\frac{3}{r}\frac{\partial Z}{\partial r}\right],$$

$Z = 0$ on L'. Now, for *any* Y this system is known to have only one solution $Z = 0$ (Courant & Hilbert 1962). Hence, $Y = A$.

Batchelor's theorem may now be applied to our problem as follows. In the limit of large Reynold's number, the viscous effects are dominant in a thin boundary layer near the liquid sheet only. Outside this boundary layer, the governing equation is well approximated by keeping only the inviscid terms of equation (6), namely

$$q_r\frac{\partial \xi/r}{\partial r}+q_z\frac{\partial \xi/r}{\partial z}=0. \tag{7}$$

This equation indicates that ξ/r is constant on each streamline. In particular, if L' denotes one such streamline along which ξ/r has the constant value A, then by Batchelor's theorem

$$\frac{\xi}{r} = A = \frac{1}{r^2}\left[\frac{\partial^2\psi}{\partial z^2} + \frac{\partial^2\psi}{\partial r^2} - \frac{1}{r}\frac{\partial\psi}{\partial r}\right] \tag{8}$$

everywhere in the region S' enclosed by L'. We shall take L' just outside the boundary layer. In this way the non-linear equation (6) may be replaced by the simpler equation (8). To be sure, the constant A must still be computed by an analysis of the boundary layer. We show in the appendix that A must be chosen so that

$$\int_0^L r^2 V v^2 ds = \int_0^L r^2 v^3 ds, \tag{9}$$

where V is the velocity of the air at the outer edge of the vortex (outside the boundary layer). The integration is carried out on the meridian limiting the water-bell. Since the pressure acting on the water-bell in the limit of large Reynold's number, depends only on the inviscid motion inside the bell our boundary value problem may be simplified: we must find a solution of (8) satisfying the condition $\psi = 0$ at the water-bell and the condition (9), together with the amended Boussinesq's equation.

4. Iterative solution

An iterative method of solution of the boundary-value problem may be readily devised. We start out with a 'convenient' choice of water-bell shape. In principle, we may obtain the solution of (8) satisfying $\psi = 0$ at the water-bell and condition (9), e.g. by the relaxation or other method. We may then calculate the pressure distribution on the water-bell by Bernoulli's equation

$$p(s) - p_{\mathrm{st}} = \tfrac{1}{2}\rho_a V^2(s), \tag{10}$$

where p_{st} denotes the stagnation pressure. p_{st} may be regarded as given since the pressure level inside the bell may be adjusted arbitrarily (e.g. see Taylor 1959). With $p(s)$ known, the ordinary non-linear differential equation (1) may be integrated numerically. In this integration we need two conditions from which the two integration constants may be determined. These are provided by the requirements that the water sheet must leave the tip of the disk in a prescribed direction at a given velocity. In this way, we compute a corrected bell shape. The procedure of calculation may now be repeated. Obviously the convergence of the iterative process and total amount of numerical computation needed for the calculation depend on the initial choice of the bell shape. If the initial shape is close to the final shape, one iteration only will be sufficient. Of course, we do not know what the final shape of the water-bell is. However, some indication of shape is provided by neglecting the pressure difference, e.g. that determined by the original Boussinesq's equation, or computed by Taylor. The size of the initial choice is not important because the pressure correction (see equation (9)) is independent of the size when the gravity effect is small (the usual case).

5. An example

The rapidity of convergence of the iterative method will now be illustrated by considering an example. We propose to compute the flow field and water-bell shape corresponding to Expt. 2 of Göring (1959). The resulting shape may then be compared directly with the experiment (dots on figure 2 indicate the shape of the water-bell in side view as measured by Göring). The magnitude and

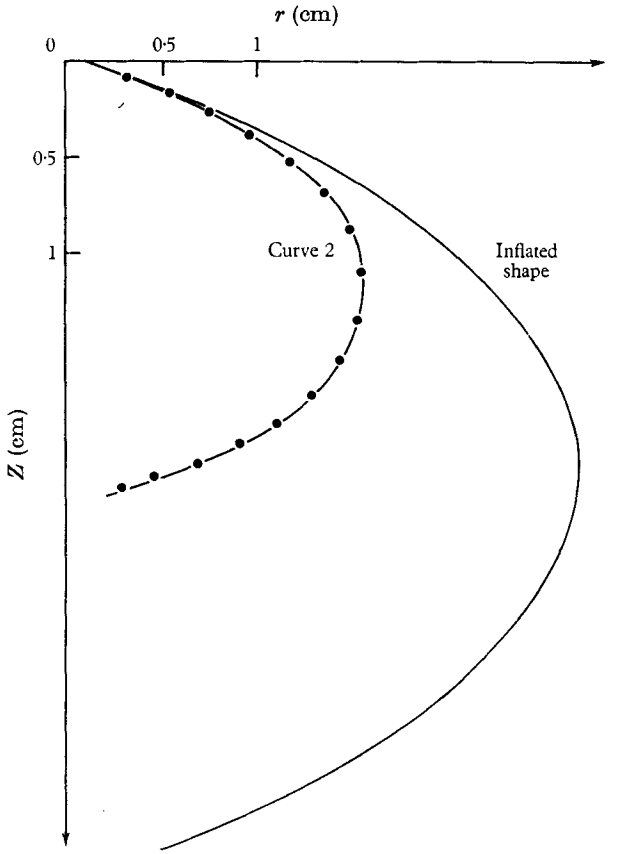

FIGURE 2. Comparison with Expt. 2. ●, experimental points. $\sin\phi_1 = 0{\cdot}940$; $v_1 = 470$ cm/sec.

direction of the water velocity leaving the disk are taken to be the same as those in the experiment ($v_1 = 470$ cm/sec, $\sin\phi_1 = 0{\cdot}940$). Moreover, we assume $p_{st} = p_0$, this assumption is reasonable as the bottom of the bell breaks easily during the experiment, in that case the stagnation pressure must always remain close to the atmospheric pressure. Let us take for initial shape a sphere of radius a. In the first iteration we may neglect the small gravity effect, in which case v is constant in (9) and the pressure correction so determined is independent of the radius a. For this reason the numerical value of a need not be specified. The solution of (8) is Hill's vortex

$$\psi = \tfrac{1}{10}Ar^2[r^2+z^2-a^2]. \tag{11}$$

Equation (9) is integrated at once to give

$$\tfrac{8}{30}Aa^2 = \tfrac{1}{2}\pi v$$

and

$$C_p = (p_0 - p)/\tfrac{1}{2}\rho_a v^2 = \tfrac{9}{64}\pi^2 \cos^2\phi, \tag{12}$$

which, of course, is independent of a, v being considered constant in equation (12) (no gravity). Using (12), we integrate equation (1) at once (see table 1), and obtain

r_{cm}	0·3	0·6	0·9	1·2	1·5	1·810
$Z_{1_{cm}}$	0·073	0·201	0·345	0·525	0·769	1·370

TABLE 1. Curve 1

$A_1 = 1077$

r_{cm}	0·3	0·6	0·9	1·2	1·5	1·810
C_{p1}	0·07	0·32	0·68	1·05	1·26	1·28

TABLE 2. Pressure correction from curve 1

r_{cm}	0·3	0·6	0·9	1·2	1·521	1·542
Z_2 (above equator)	0·072	0·198	0·346	0·553	1·112	1·199
Z_2 (below equator)	2·236	2·139	1·991	1·791	1·278	1·199
Z exp. (above equator)	0·072	0·196	0·345	0·558	1·190	—
Z exp. (below equator)	2·218	2·121	1·972	1·782	1·190	—

TABLE 3. Curve 2 and experimental results

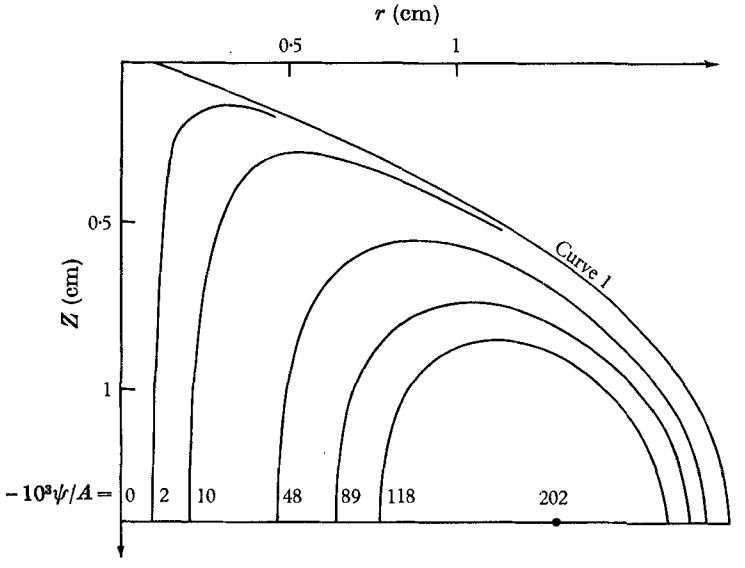

FIGURE 3. Solution of equation (8) for curve 1, by relaxation method.

curve 1 in figure 3. We repeat the procedure with curve 1, but now equation (8) with condition (9) have to be solved numerically. In figure 3 we also represent a few curves $\psi/A = \text{const.}$, as obtained by the method of relaxation. Then we deduce A and $C_p = (p_0 - p)/\frac{1}{2}\rho_a v_e^2$, see table 2. v_e is the velocity of the water at the equator of curve 1 (we keep the small correction due to gravity). Integration of equation (1) once more leads to curve 2 in figure 2, see table 3. No experimental point is at a distance from curve 2 larger than 1 % of the bell diameter. Repetition of the procedure with curve 2 yields no appreciable change in shape. In the tables only a few representative values are given. Points below the equator are not exactly symmetric to those above, the difference is due to the variation of v with gravity.

Two results are apparent from the numerical analyses: our iterative scheme converges rapidly; one could, of course, obtain a numerical solution within any accuracy with more than two iterations. The numerical analysis shows also that the solution agrees well with the experimental points.

6. Approximate method

While a solution exact up to any desired precision may be computed by the iterative method, it is possible to devise approximate solutions which give good agreement with the experiments.

Beginning with a sphere, we may compute curve 1 as in the last section. Once we obtain curve 1, we may try to compute the new pressure correction not with curve 1 but with a curve close to it. Hence we may choose a shape for which a closed form analytic solution of equation (8) is known. Many such solutions can be constructed easily. Two are found to be of interest in the present problem. If the shape is the ellipsoid of revolution with major axis a and minor axis b, it is easy to verify that the solution of equation (8) satisfying $\psi = 0$ at the wall is

$$\psi = \frac{Ar^2}{8/a^2 + 2/b^2}\left[\frac{r^2}{a^2} + \frac{z^2}{b^2} - 1\right]. \tag{13}$$

If an onion shape is desired, another solution may be helpful,

$$\psi = \frac{Ar^2}{8 + 16ab/3}[r^2(za+1) - \tfrac{4}{3}az(z-b)^2]. \tag{14}$$

It is found in general that ellipsoids are better for high velocities when gravity effects are small. Onion shapes are more appropriate for low velocity when points below the equator are quite unsymmetric of those above.

r_{cm}	0·3	0·6	0·9	1·2	1·5	0·810
C_p	0·08	0·31	0·63	0·96	1·15	1·16

TABLE 4. Pressure correction for ellipse
$a = 1{\cdot}81$ cm $b = 1{\cdot}07$ cm, $A = 1023$

In both cases there are still two parameters a and b which may be assigned arbitrarily. For example, let us consider again curve 1 and approximate it by an ellipse having the same diameter and same radius of curvature at the equator. We can repeat the integration procedure with the ellipse, analytically.

From equation (13) one can show easily that

$$C_p = \frac{p_0 - p}{\frac{1}{2}\rho_a v^2} = \left(\frac{V_e}{v}\right)^2 \frac{r^2}{b^2}\left[1 - \frac{r^2}{a^2}k^2\right], \tag{15}$$

where V_e is the air speed at the equator with

$$V_e = a^2 b^2 A/(4b^2 + a^2)$$

and

$$k^2 = (a^2 - b^2)/a^2.$$

Equation (9) can be integrated at once to give A (or V_e)

$$\frac{v_e}{3k^2k'^2}[k'^2K + (2k^2 - 1)E] = \frac{V_e a}{b^3}\left[\frac{a^2 + b^2}{3} - \frac{a^2 - b^2}{5}\right], \tag{16}$$

with standard notations for elliptic integrals (Jahnke & Emde 1945). To derive (16), we took $v = v_e$, the error in doing so is negligible.

Table 4 gives the pressure coefficient C_p at the meridian computed for the ellipse. Using those values in (1) we obtain by numerical integration a new curve which agrees with curve 2, within 2 %.

In figure 2 we also draw the inflated shape obtained by neglecting the pressure correction altogether in (1). Instead of starting with a sphere one could have used this curve for initial shape. Using only the approximate method (with an ellipse) for simplicity, we obtain a curve which agrees with curve 2, within 2 %. Only one iteration is needed here, again this was expected since the inflated shape is roughly similar to the final one. The approximate method predicts the proper shape and is quite easy to apply since no numerical solutions of (8) and (9) are needed.

7. Further comparisons with experiments and conclusions

Three other experiments of Göring (1959) (Expts. 1, 3, 5) are also available to check our theory. The magnitude and direction of the water velocity leaving the disk are indicated for each experiment in figures 4, 5, 6. The largest effect due to internal air motion occurs when the water velocity has its highest value. This is the case of Expt. 2 which we considered earlier with some detail as it provides the most crucial test of our theory. The iterative procedure is easily repeated for Expts. 1, 3, 5 and the results are represented in figures 4, 5, 6. The dots are the experimental points; curve 2 again represents the final theoretical result; the inflated shape is obtained by neglecting the pressure correction. Convergence and precision are those found in the case of Expt. 2. We obtain similar results by using the approximate method.

In conclusion we find that our theory, whether numerical and exact or partly analytical and approximate, agrees well with the experiments. Previous investigators who used the water-bell experiment neglected the air motion in the cavity. Comparing the inflated shape with the actual shape gives the error of that omission (which naturally is highest for Expt. 2).

After completion of the manuscript our attention was brought to papers by O'Brien (1961) and Burggraf (1966) which have some bearing on the present problem.

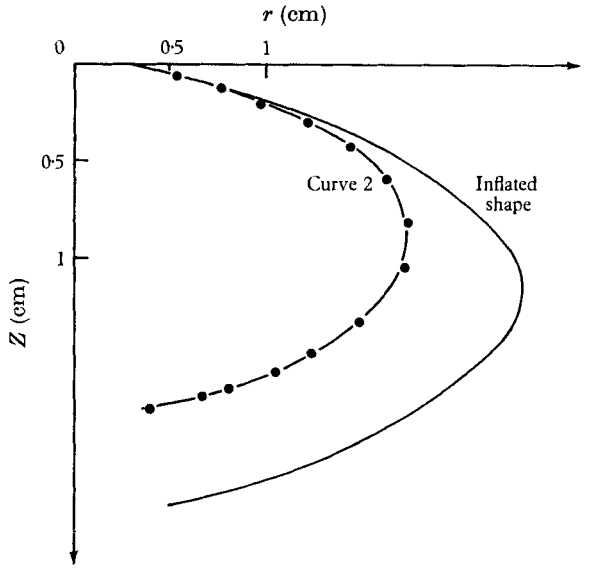

FIGURE 4. Comparison with Expt. 1. ●, experimental points
$\sin \phi_1 = 0{\cdot}970$; $v_1 = 337$ cm/sec.

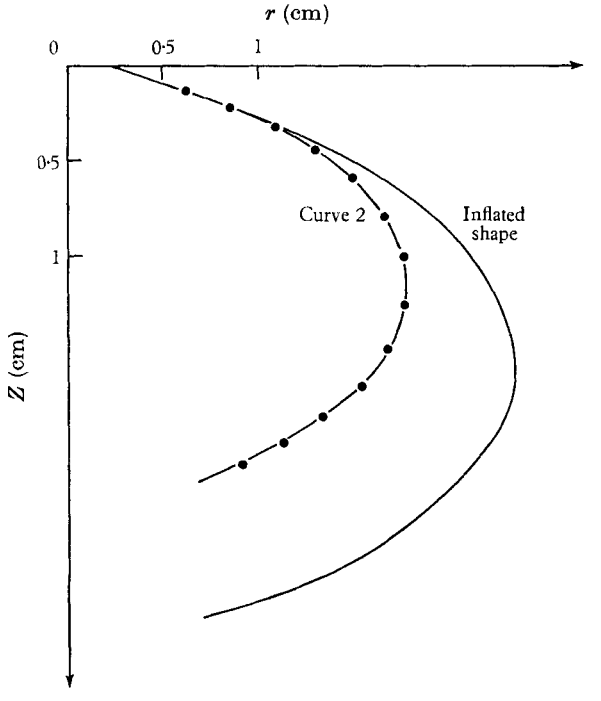

FIGURE 5. Comparison with Expt. 3. ●, experimental points.
$\sin \phi_1 = 0{\cdot}964$; $v_1 = 374$ cm/sec.

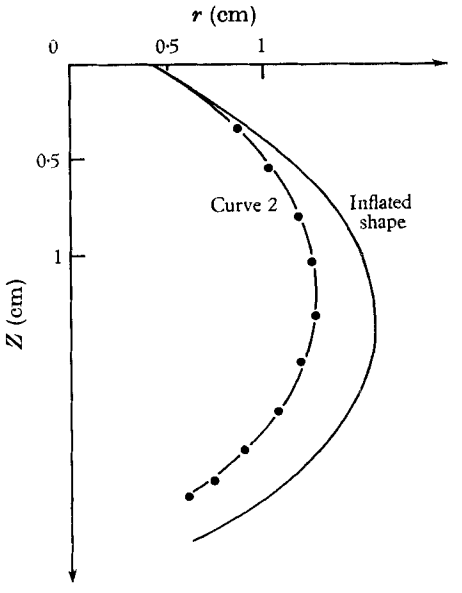

FIGURE 6. Comparison with Expt. 5. ●, experimental points. $\sin\phi_1 = 0{\cdot}844$; $v_1 = 283$ cm/sec.

The author wishes to acknowledge helpful discussions with Professors Peter P. Wegener and B. T. Chu of Yale University and the receipt of original data provided by Dr Wolfgang Göring. The support of the Power Branch of the U.S. Office of Naval Research is also gratefully acknowledged.

Appendix

Between the wall and the outer edge of the vortex there is a boundary layer. Its study will show how to relate, in general, $v(s)$ and A. Using the von Mises equation, Wood (1957) determined such a relation for the two-dimensional case. We shall operate in a similar manner for the axisymmetric case. Inside the boundary layer, we have

$$V\frac{\partial V}{\partial s}+\frac{1}{\rho_a}\frac{dp}{ds}=\nu_a r V\frac{\partial}{\partial\psi}\left(rV\frac{\partial V}{\partial\psi}\right).$$

Integrating this equation over any streamline inside the boundary layer, we obtain

$$\int rV\frac{\partial}{\partial\psi}\left(rV\frac{\partial V}{\partial\psi}\right)ds=0.$$

One part of the streamline lies on the axis where $r=0$ and another under the disk where $V\simeq 0$, hence, both parts contribute nothing to the integral. Only the portion of the streamline next to the water sheet (outside the disk) has to be considered and there the velocity V should be rather close to the water velocity $v(s)$. Then, let us assume that

$$V=v(s)+\overline{V},\quad\text{with}\quad|\overline{V}|\ll|v(s)|.$$

We can linearize the integral and keeping only the first-order term, write:

$$\int_0^L r^2 v(s)^2 \frac{\partial^2 \overline{V}}{\partial \psi^2} ds = 0,$$

which can also be written

$$\frac{\partial}{\partial \psi} \int_0^L r^2 v(s)^2 \frac{\partial \overline{V}}{\partial \psi} ds = 0.$$

In doing so, we neglected a term $(\partial L/\partial \psi)\, r^2 v(s)^2 (\partial \overline{V}/\partial \psi)$; one checks easily from its order of magnitude that it is negligible in the boundary layer. Then

$$\int_0^L r^2 v(s)^2 \frac{\partial \overline{V}}{\partial \psi} ds = \text{const.},$$

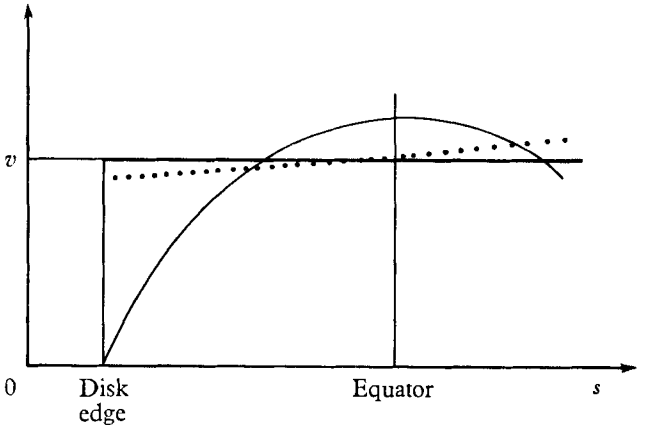

FIGURE 7. Sketch of velocities: —, water velocity (no gravity); · · ·, water velocity (with gravity); —, velocity at the outer edge of the vortex.

the constant has to be zero, since it is the value of the integral at the outer edge of the vortex. Repeating the process, we get

$$\int_0^L r^2 v(s)^2 \, \overline{V} \, ds = \text{const.}$$

The constant in the last equation is zero (value for the streamline touching the water) or

$$\int_0^L r^2 v(s)^2 \, V \, ds = \int_0^L r^2 v(s)^3 \, ds. \tag{A 1}$$

If we take for V the velocity at the outer edge of the vortex $V(s)$, we have

$$\int_0^L r^2 \, V(s) \, v^2(s) \, ds = \int_0^L r^2 v^3(s) \, ds, \tag{A 2}$$

which is equation (9). If gravity is negligible then $v(s) = \text{const.}$ and

$$\int_0^L r^2 V(s) \, ds = v \int_0^L r^2 \, ds, \tag{A 3}$$

$v(s)$ is known from experiments and $V(s)$ from equation (8). Then from equation (A 2) we get an expression for A. Finally, figure 7 shows a typical plot for $V(s)$ and $v(s)$ on the meridian. Obviously, the assumption of linearity is appropriate.

REFERENCES

BATCHELOR, G. K. 1956 On steady laminar flow with closed streamline at large Reynolds number. *J. Fluid Mech.* **1**, 177.

BOUSSINESQ, J. 1913 Sur la théorie des nappes liquides rétractiles de Savart. *Comptes Rendus* **157**, 89.

BURGGRAF, O. R. 1966 Analytical and numerical studies of the structure of steady separated flows. *J. Fluid Mech.* **24**, 113.

COURANT, R. & HILBERT, D. 1962 *Methods of Math. Physics*, Vol. II, 320. NewYork: John Wiley and Sons.

GÖRING, W. 1959 Zur Abhängigkeit der Oberflächenspannung von der Bildungs—und Alterungsgeschwindigkeit der Oberfläche. *Z. Elektrochem., Ber. Bunsenges. physik. Chem.* **63**, 1069.

JAHNKE, E. & EMDE, F. 1945 *Tables of Functions*. New York: Dover.

O'BRIEN, V. 1961 Steady spheroidal vortices—more exact solutions of the Navier-Stokes equation. *Quart. Appl. Math.* **19**, no. 2, 163.

TAYLOR, SIR GEOFFREY. 1959 The dynamics of thin sheets of fluid. I. Water bells. *Proc. Roy. Soc.* A **253**, 289.

WEGENER, P. P. & PARLANGE, J.-Y. 1964 Surface tension of liquids from water-bell experiments. *Z. für Physikalische Chemie (Neue folge)* **43**, 245.

WOOD, W. W. 1957 Boundary layers whose streamlines are closed. *J. Fluid Mech.* **2**, 77.